Available online at www.sciencedirect.com
ScienceDirect
Journal of Colloid and Interface Science 321 (2008) 393–400
JOURNAL OF Colloid and Interface Science
www.elsevier.com/locate/jcis

Constitutive modeling of contact angle hysteresis

Srikanth Vedantam [a,*], Mahesh V. Panchagnula [b]

[a] Department of Mechanical Engineering, National University of Singapore, Singapore 117576
[b] Department of Mechanical Engineering, Tennessee Technological University, TN 38505, USA

Received 5 December 2007; accepted 29 January 2008
Available online 20 February 2008

Abstract

We introduce a phase field model of wetting of surfaces by sessile drops. The theory uses a two-dimensional non-conserved phase field variable to parametrize the Gibbs free energy of the three-dimensional system. Contact line tension and contact angle hysteresis arise from the gradient term in the free energy and the kinetic coefficient respectively. A significant advantage of this approach is in the constitutive specification of hysteresis. The advancing and receding angles of a surface, the liquid–vapor interfacial energy and three-phase line tension are the only required constitutive inputs to the model. We first simulate hysteresis on a smooth chemically homogeneous surface using this theory. Next we show that it is possible to study heterogeneous surfaces whose component surfaces are themselves hysteretic. We use this theory to examine the wetting of a surface containing a circular heterogeneous island. The contact angle for this case is found to be determined solely by the material properties at the contact line in accord with recent experimental data.

Keywords: Wetting; Contact angle; Hysteresis; Heterogeneous; Phase field theory

1. Introduction

Wetting of surfaces by liquid drops has been studied for over two centuries starting with Young in 1805. The associated phenomena are still of significant current interest due to the many technological applications. A major result of Young [1] relating the contact angle of a drop (θ_Y) to the solid–liquid (γ_{SL}), liquid–vapor (γ_{LV}) and solid–vapor (γ_{SV}) surface energies,

$$\cos\theta_Y = \frac{\gamma_{SV} - \gamma_{SL}}{\gamma_{LV}}, \tag{1}$$

pertains to the equilibrium state of the drop. Young's equation (1) which neglects the solid–liquid–vapor three-phase contact line tension was modified by Boruvka and Neumann [2] as

$$\cos\theta'_Y = \cos\theta_Y - \frac{\tau\mathcal{K}}{\gamma_{LV}}, \tag{2}$$

where τ is the three-phase contact line tension and $\mathcal{K}$ is the curvature. The contact angle of the drop obtained from these theories is the equilibrium contact angle on a smooth, chemically homogeneous surface. For heterogeneous surfaces, Cassie [3] derived the equation for the equilibrium contact angle

$$\cos\theta_Y^C = f^A\cos\theta_Y^A + f^B\cos\theta_Y^B, \tag{3}$$

in terms of the equilibrium contact angles (θ_Y^i) and area fractions (f^i) of the component surfaces ($i = A, B$); for a smooth surfaces $f^A + f^B = 1$. On the other hand, for a rough homogeneous surface, Wenzel [4,5] derived the equation

$$\cos\theta_Y^W = r\cos\theta_Y, \tag{4}$$

where r is the roughness factor (ratio of the actual area to the projected area of the surface).

The equilibrium contact angle is rarely observed experimentally *even for smooth homogeneous surfaces*. Instead the measured contact angle of a sessile drop usually lies in a range $\theta_r \leqslant \theta \leqslant \theta_a$ bounded by the receding and advancing angles θ_r and θ_a respectively. The advancing and receding angles are empirically reproducible and the contact angle hysteresis (CAH) $\Delta\theta = \theta_a - \theta_r$ is a characteristic describing surface wettability.

The origin of CAH has been the subject of vigorous debate for over thirty years now. Some important causes that have been shown to affect the hysteretic behavior of a sessile drop

* Corresponding author. Fax: +65 6779 1459.
E-mail address: srikanth@nus.edu.sg (S. Vedantam).

0021-9797/$ – see front matter
doi:10.1016/j.jcis.2008.01.056

are surface roughness, chemical heterogeneities and presence of solutes in the liquid [6,7]. The relative contributions of these factors to the total CAH depends on the system being considered. In addition, Yang [8] and Extrand [9] have shown that the irreversible adhesion and separation events that occur during the advancing and receding processes contribute to hysteresis. The creation of bonds during the advancing process and their destruction during the receding process are inherently irreversible due to the dispersion of energy from the interface through atomic vibration (analogous to crack growth in solids). These effects on atomically smooth and chemically homogeneous defect free surfaces have been experimentally demonstrated by Chen et al. [10] and Extrand and Kumagai [11] as well as through molecular dynamics simulations by Freund [12]. Roughness, chemical heterogeneities, solutes, surface deformation, liquid absorption and retention, molecular rearrangement upon wetting, and interdiffusion may be other factors that *augment* this fundamental cause.

Most theoretical models till date have focused on surface roughness and heterogeneities as the source of CAH. The first models studied idealized surfaces with periodic roughness in the form of parallel grooves [13,14] or axisymmetric grooves [15]. Later models were used to obtain the contact angle for smooth but heterogeneous surfaces [16,17]. Subsequently, models of surfaces with randomly distributed defects invoked pinning of the three-phase contact line to study CAH [18,19]. Further, explicit consideration of the three-phase contact line pinning due to defects allowed random distribution of defects to be studied in a statistical manner [20]. A thermodynamic model combining surface roughness and heterogeneities has also been proposed [21]. Hysteresis on smooth homogeneous surfaces has been addressed theoretically by [22] as a consequence of the shape of disjoining isotherms.

There have been several numerical approaches to studying wetting of surfaces. Schwartz [23] proposed a lubrication model of the Navier–Stokes equations. Several researchers [24–27] have used the *Surface Evolver* program for minimization of surface energy of the drop to obtain realistic drop shapes on heterogeneous surfaces. Porcheron and Monson [28] studied the Wenzel and Cassie states using a lattice gas model. Most recently, Kusumaatmaja and Yeomans [29] have presented a lattice Boltzmann solution of the Navier–Stokes equations coupled with the minimization of a free surface energy functional to model sessile drops on heterogeneous surfaces. The approaches described above are useful for developing fundamental understanding of sessile drop behavior on heterogeneous surfaces. However, they have one serious physical limitation in that the smooth, chemically homogeneous, component surfaces are assumed to be free of hysteresis. Hysteresis of component materials has been shown to impact the macroscopic sessile drop behavior [30]. Our proposed approach allows a thermodynamically consistent method of incorporating hysteresis on smooth surfaces into models of sessile drops, thereby enhancing their applicability.

In all the above models, the specific geometry of the surface roughness and the distribution of chemical heterogeneities is assumed and the source of hysteresis is limited to these two mechanisms in spite of the fact that other mechanisms have also been shown to be important. Furthermore, even if chemical heterogeneities are solely responsible for hysteresis and the component surfaces are hysteresis free, it is in practice extremely difficult to obtain the component surface equilibrium angles in many instances. To take an example which we will study further in this paper, Extrand [31] reports CAH of 23 degrees for PFA and 55 degrees for etched PFA with similar roughness values for the two materials. The etching process strips the fluorine molecules from the carbon in PFA and the surface reacts with oxygen, water vapor and hydrogen in some random manner when exposed to air. To obtain the "component" surface equilibrium angles and model the distribution of heterogeneities in this case is clearly impractical.

Thus due to practical considerations, it seems desirable to develop a phenomenological model which incorporates hysteresis without explicit consideration of the source. Our model is a constitutive approach analogous to, for example, the Hooke's law for elastic solids. While the origin of elasticity may be due to different causes in metals and polymers, the same constitutive form of the equation is used. Similarly, provided constitutive information about the advancing and receding angles, our model describes wetting of surfaces regardless of the origin of the hysteresis.

In this paper, we present such a phenomenological theory which describes the equilibrium aspects embodied in Eqs. (1) and (2) as well as kinetic aspects of CAH independent of the physical origins. The theory is developed in a Ginzburg–Landau (GL) framework and uses a phase field to describe the amount of wetting at each point on the solid surface. Previously, phase field models have been used successfully to describe solid–liquid phase transitions [32] and solid–solid phase transitions (e.g., ferroelectric, martensitic transitions [33]). In the current model, we treat the motion of the sessile drop as causing a "phase transition" of the solid surface between wetted and non-wetted "phases." The theory consists of two essential features: a free energy functional and an evolution equation for the phase field variable. The free energy functional is composed of a coarse grained free energy function and a gradient energy term. The coarse grained energy accounts for the surface energy contributions of the solid–liquid, liquid–vapor and solid–vapor interfaces. The gradient term accounts for the three-phase contact line tension. We focus purely on quasistatic drop motion in this paper and neglect hydrodynamic effects. The instantaneous shape and contact angle, θ, of the sessile drop is computed from an evolution equation which is capable of taking the metastable nature of drop states with $\theta_r \leqslant \theta \leqslant \theta_a$ into account.

We would like to emphasize an important aspect of this theory. The only constitutive inputs for this theory are: (i) the advancing and receding angles, (ii) the surface energy of the liquid–vapor interface, and (iii) the line tension coefficient; all of which are physically meaningful parameters. Using these inputs, GL theory provides a simple, thermodynamically consistent means of incorporating hysteresis. An immediate possible application could be to study wetting of *composite* surfaces whose component surface hysteresis is constitutively prescribed. Since the line tension is incorporated in a natural man-

ner, the interaction of the contact line with the heterogeneities can be studied. To the best of our knowledge, this is the only such model capable of constitutively incorporating hysteresis to date.

Our focus in this work is twofold: (1) we describe the essential features of the phase field model applied to the problem of wetting by sessile drops and (2) we demonstrate how the material properties at the *three-phase contact line* affect the contact angle [34]. The main advantage of this model is the ease with which topographical and chemical heterogeneities can be incorporated in a phenomenological fashion. We discuss the effect of roughness in the context of the Wenzel equation (4) and how our model can incorporate hysteresis on a arbitrary roughness. Next, we study the effect of heterogeneous chemical properties in an axisymmetric setting and show that our theory describes the phenomena presented experimentally by Extrand [31]. Similar experiments [35,36] showing the effect of surface roughness at the contact line will not be discussed here but can be described by the theory in an entirely analogous manner. Elsewhere we present the consequences of contact line contortions on the contact angle on two-dimensional heterogeneous surfaces [37]. Since the wetting–dewetting transformation is modeled through the three-phase contact line kinetics in the current phase field description, Cassie–Wenzel transition would also be restricted to the contact line [38,39].

2. Theory

The basic feature of the phase field theory is a two-dimensional field variable (order parameter) $\eta(\mathbf{x}, t)$ which represents the wetted state of the solid surface. The phase field variable is assumed to take a value 1 (say) where the liquid drop is in contact with the solid surface and 0 (say) where the solid surface is in contact with the vapor. The phase field variable undergoes smooth but steep transitions (see, for example, Fig. S1 of supporting material) between the wetted and non-wetted regions on the solid surface. Since our order parameter describes the amount of wetting of the solid surface, we are able to use a non-conserved phase field variable in contrast to [40] in which a three-dimensional conserved order parameter describes the volume of the liquid.

Our aim is to parametrize the full three-dimensional system Gibbs free energy,

$$\mathcal{G} = \gamma_{\mathrm{SL}} A_{\mathrm{SL}} + \gamma_{\mathrm{LV}} A_{\mathrm{LV}} + \gamma_{\mathrm{SV}} A_{\mathrm{SV}}, \tag{5}$$

using the phase field variable $\eta(\mathbf{x}, t)$. In other words, we seek a function $f(\eta)$ such that $\mathcal{G} = \int_A f(\eta)\, dA$ where the domain of integration is the entire *solid surface area*. In order to construct our free energy function $f(\eta)$, it is instructive to view the free energy as $\mathcal{G} = \int_{A(\eta=0)} f(0)\, dA + \int_{A(\eta=1)} f(1)\, dA + \int_{A(0<\eta<1)} f(\eta)\, dA$, where $A(\eta = 0)$ and $A(\eta = 1)$ represent the area of the non-wetted ($\eta = 0$) and wetted ($\eta = 1$) regions of the solid surface respectively. In the phase field theory the transition region is finite though small. Purely for the purpose of comparison of the energy of the phase field model to Eq. (5) we consider the limit of vanishing interface thickness in which case $A(0 < \eta < 1) = 0$. Then the term $\int_{A(\eta=0)} f(0)\, dA$ represents the solid–vapor contribution $\gamma_{\mathrm{SV}} A_{\mathrm{SV}}$ and $\int_{A(\eta=1)} f(1)\, dA$ represents solid–liquid and liquid–vapor contribution to the Gibbs free energy: $\gamma_{\mathrm{LV}} A_{\mathrm{LV}} + \gamma_{\mathrm{SL}} A_{\mathrm{SL}}$.

Since $\eta = 0$ represents the non-wetted regions (solid surface in contact with vapor) on the solid surface, we choose $f(0) = \gamma_{\mathrm{SV}}$. Where $\eta = 1$, the liquid drop is in contact with the solid surface. Therefore, $f(1)$ is required to provide the liquid–vapor *and* the solid–liquid interfacial energy contributions. We achieve this by associating the interfacial energy of an elemental liquid–vapor area to an elemental liquid–solid area on the solid surface. Note from Eq. (5) that the surface energy components must be multiplied by the appropriate surface areas while the domain of integration of $f(\eta)$ is only the solid surface area. This can be accounted for by assuming the shape of the liquid drop to be a spherical cap (appropriate for drops of radius smaller than the capillary length under quasistatic advancing or receding conditions). For a drop of spherical cap shape, the volume of the drop V is related to the wetted circle radius R and the contact angle θ through

$$V = \frac{1}{3}\pi R^3 \frac{(2 - 3\cos\theta + \cos^3\theta)}{\sin^3\theta}. \tag{6}$$

The liquid–vapor surface area of the drop is given by $A_{\mathrm{LV}} = 2\pi R^2(1 - \cos\theta)/\sin^2\theta$ and the solid–liquid surface area is given by $A_{\mathrm{SL}} = \pi R^2$. Thus the elemental liquid–vapor surface area is given by

$$dA_{\mathrm{LV}} = 4\pi R \frac{(1 - \cos\theta)}{\sin^2\theta}\, dR + 2\pi R^2 \left(\frac{1}{\sin\theta} - \frac{\sin\theta}{1 + \cos\theta} \right) d\theta \tag{7}$$

and the elemental solid–liquid area is

$$dA_{\mathrm{SL}} = 2\pi R\, dR. \tag{8}$$

Differentiating Eq. (6) at constant volume we obtain $R\, d\theta = -2(\sin\theta + \sin 2\theta/4)\, dR$. Substituting for $d\theta$ in Eq. (7) we obtain

$$dA_{\mathrm{LV}} = dA_{\mathrm{SL}} \cos\theta. \tag{9}$$

It has to be emphasized that Eq. (9) is not a trigonometric relationship but one that arises from association of elemental areas gained or destroyed under the constraint of constant volume. Thus if we choose $f(1) = \gamma_{\mathrm{SL}} + \gamma_{\mathrm{LV}} \cos\theta$, the integral of $f(1)$ over the wetted surface area includes the solid–liquid and liquid–vapor contributions of the free energy. Without loss of generality, we shift the reference energy and conveniently choose $f(0) = 0$ and $f(1) = \gamma_{\mathrm{SL}} + \gamma_{\mathrm{LV}} \cos\theta - \gamma_{\mathrm{SV}}$.

It is worth noting that surface roughness can be incorporated by scaling the surface areas by r, the ratio of the actual area to the projected area. Thus, in general, $f(1) = r(\gamma_{\mathrm{SL}} - \gamma_{\mathrm{SV}}) + \gamma_{\mathrm{SL}} \cos\theta$. This form is used in the discussion of the Wenzel equation (4). For the rest of the paper, we focus on chemical heterogeneities and ignore the roughness factor by setting $r = 1$.

We next require $f(\eta)$ to reflect the fact that the wetted and non-wetted regions of the solid surface may be stable or metastable states. Here we use "metastable" to describe a drop

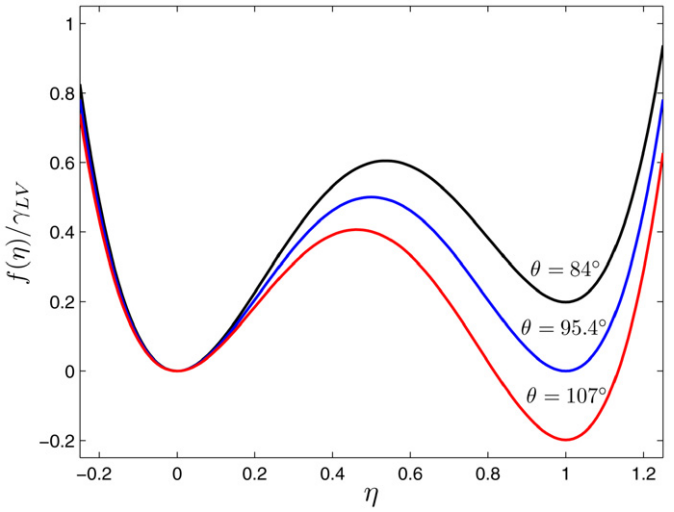

Fig. 1. Double-well potential $f(\eta)/\gamma_{LV}$ for three contact angles.

state that corresponds to a local minimum of the free energy function which is different from the global minimum. All other states of η should be unstable. Further, the exact shape of the double-well potential affects the equilibrium shape of the interface between the wetted and non-wetted regions but not the kinetics or the location of the interface.

The required properties for f described above can be obtained by choosing $f(\eta)$ to take a double-well form with local minima at $\eta = 0, 1$. The fine structure of the interface does not affect the equilibrium results as described above and so we choose a simple double-well form for $f(\eta)$ as a quartic function of η,

$$f(\eta) = \gamma_{LV}\{8\eta^4 - 2(H+8)\eta^3 + (3H+8)\eta^2\}, \tag{10}$$

where we have set $H = (f(1) - f(0))/\gamma_{LV} = \cos\theta - \cos\theta_Y$ using Eq. (1). Fig. 1 shows the plot of $f(\eta)/\gamma_{LV}$ for three different values of the contact angle. The equilibrium Young's angle for the material is given by the average of the cosines of the advancing and receding angles $\theta_Y = \cos^{-1}(\frac{1}{2}(\cos\theta_a + \cos\theta_r)) = 95.4°$, using typical values for a perfluoroalkoxy (PFA) film-coated substrate [31]. H represents the imbalance in the capillary forces and is the difference in heights of the two minima at $\eta = 0, 1$. As can be seen from Fig. 1, for $\theta < \theta_Y$, the $\eta = 1$ minimum is metastable and the drop attempts to retreat into a smaller wetted circle while aspiring to reach the Young's equilibrium condition. Whereas the $\eta = 0$ well is metastable when $\theta > \theta_Y$ with the drop attempting to wet additional solid surface in order to reach the Young's equilibrium condition. It can therefore be seen that when the non-wetted and wetted regions are both stable ($f(1) = f(0)$), Young's equation (1) is obtained.

The total free energy for the phase field model is written as

$$\mathcal{F} = \int_A \left(f(\eta) + \frac{1}{2}\lambda|\nabla\eta|^2 \right) dA. \tag{11}$$

The gradient term provides a penalty for the presence of interfaces between $\eta =$ constant regions, which, in the current context, is the three-phase contact line tension associated with the solid–liquid–vapor contact line. It has been postulated that this line tension arises out of finite range molecular forces at the contact line [41]. The gradient coefficient λ (thermodynamically required to be positive) is shown below to be related to the three-phase contact line tension. Equation (11) is the phase field equivalent of the Gibbs free energy expression (5) and includes the energy of the three-phase contact line.

In the Ginzburg–Landau framework of the phase field theory, the equilibrium solution for the order parameter is obtained through a gradient flow evolution equation of the form

$$\beta\dot{\eta} = -\frac{\delta\mathcal{F}}{\delta\eta} = \lambda\nabla^2\eta - \frac{\partial f(\eta)}{\partial\eta}, \tag{12}$$

where δ is a functional derivative and $\beta(\mathbf{x}, t, \eta, \nabla\eta, \dot{\eta}) > 0$ is the kinetic coefficient which is required to be positive for all admissible values of its arguments [42]. It is worth remarking that in regions away from the three-phase contact line, where $\eta = 0$ or 1, both terms on the right-hand side of Eq. (12) vanish and there is no evolution of η. Thus the evolution of the drop radius is only through the motion of the contact line and the local material properties at the contact line determine the state of the drop. This is physically consistent with thermodynamic energy minimization principle that the *change* in free energy determines the state of the drop [34].

When the drop is axisymmetric, the Ginzburg–Landau equation (12) becomes

$$\beta\dot{\eta} = \lambda\left(\frac{\partial^2\eta}{\partial r^2} + \frac{1}{r}\frac{\partial\eta}{\partial r} \right) - \frac{\partial f}{\partial\eta}, \tag{13}$$

where r is the radial coordinate measured from the center of the wetted circle. Assuming for the moment that $\beta =$ constant and the boundary conditions for a drop of radius R to be

$$\begin{aligned} &\eta = 1, \quad \frac{\partial\eta}{\partial r} = 0, \quad \text{at } r = 0, \\ &\eta = 0, \quad \frac{\partial\eta}{\partial r} = 0, \quad \text{at } r = \infty, \end{aligned} \tag{14}$$

it is instructive to integrate (13) from $0 < r < \infty$ to obtain

$$\alpha\beta v = f(0) - f(1) - \frac{\alpha\lambda}{R}. \tag{15}$$

Here v is the velocity of $\eta =$ constant surfaces (contact line velocity) and $\alpha = \int_0^\infty (\partial\eta/\partial r)^2\, dr$ [43]. Equation (15) is the sharp interface analog of the phase field equation (13) [42,44–46]. Substituting for $f(0)$ and $f(1)$, and identifying $\tau = \alpha\lambda$, Eq. (15) for a stationary interface ($v = 0$) gives the modified Young's equation [2].[1] It may also be noted from Eq. (15) that thermodynamic equilibrium condition is only realized under quasistatic conditions ($v = 0$). However, the current phase field model is capable of handling finite contact line velocity situations although we restrict our current study to quasistatic drop evolution. Thus the evolution of the interface is curvature driven and the effect of the line tension is naturally accounted for by the gradient term. We note that since the gradient coefficient

[1] If the roughness factor is taken into consideration as discussed in the paragraph following Eq. (9), Wenzel's equation (4) modified by line tension is obtained.

is required to be positive in our theory, we cannot treat negative line tensions reported in the literature (e.g., Pompe and Herminghaus [41]). In order to study the effect of negative line tension a three-dimensional description may be required.

From Eq. (15), if the contact angle of a drop advancing with a velocity v is θ_a and receding with velocity $-v$ is θ_r, the CAH at a particular drop radius is given by

$$\cos\theta_a - \cos\theta_r = 2\alpha\beta v. \tag{16}$$

It is seen from Eq. (16) that the CAH vanishes for $v \to 0$. In addition, Eq. (16) also suggests that CAH is proportional to the velocity [47]. Experimental evidence however indicates that CAH is non-zero for negligibly small contact line velocities and is also independent of v over two orders of magnitude [7,11]. Therefore the CAH obtained with a constant kinetic coefficient is not consistent with empirical observations. We observe from Eq. (16) that a term which is proportional to $1/v$ in β may be required for non-zero CAH to be obtained as $v \to 0$.

In order to account for finite and rate-independent hysteresis for small advancing and receding drop velocities, we choose a more general form for the kinetic coefficient [48]:

$$\beta = \big(\delta\mathcal{H}\big(|\nabla\eta|\big) + \omega|\dot{\eta}|^m\big)\big/|\dot{\eta}|, \quad \delta, \omega > 0. \tag{17}$$

We have used the notation $\mathcal{H}(|\nabla\eta|)$ to represent the function $\mathcal{H}(x) = 1$ for $x > 0$ and $\mathcal{H}(x) = 0$ for $x \leqslant 0$. The δ term provides the rate-independent contribution of the hysteresis and $\omega|\dot{\eta}|^m$ provides a power law dependence of the hysteresis. In addition, the new form of the kinetic coefficient describes the intermediate kinetic states of the drop in a hysteretic system. Substituting the general form in an axisymmetric setting into (13) gives

$$\left(\delta\mathcal{H}\left(\left|\frac{\partial\eta}{\partial r}\right|\right) + \omega|\dot{\eta}|^m\right)\operatorname{sgn}(\dot{\eta}) = \lambda\left(\frac{\partial^2\eta}{\partial r^2} + \frac{1}{r}\frac{\partial\eta}{\partial r}\right) - \frac{\partial f}{\partial\eta}, \tag{18}$$

where we use $\operatorname{sgn}(S)$ to denote the sign of S. Taking the sign of both sides of Eq. (18), we see that $\operatorname{sgn}(\dot{\eta}) = \operatorname{sgn}(\lambda\partial^2\eta/\partial r^2 + (\lambda/r)\partial\eta/\partial r - \partial f/\partial\eta)$. After some algebraic manipulation, (18) can be rewritten as

$$\dot{\eta} = \begin{cases} \mathcal{W}^{1/m}\operatorname{sgn}\big(\lambda\frac{\partial^2\eta}{\partial r^2} + \frac{\lambda}{r}\frac{\partial\eta}{\partial r} - \frac{\partial f}{\partial\eta}\big), & \mathcal{W} > 0, \\ 0, & \mathcal{W} \leqslant 0, \end{cases} \tag{19}$$

where we have set

$$\mathcal{W} = \frac{1}{\omega}\left(\left|\lambda\left(\frac{\partial^2\eta}{\partial r^2} + \frac{1}{r}\frac{\partial\eta}{\partial r}\right) - \frac{\partial f}{\partial\eta}\right| - \delta\mathcal{H}\left(\left|\frac{\partial\eta}{\partial r}\right|\right)\right).$$

$\mathcal{W} \leqslant 0$ indicates the metastable drop contact angle states $\theta_r \leqslant \theta \leqslant \theta_a$. From the above equation it can be seen that δ represents the hysteresis and is given by $\delta/\gamma_{LV} = \frac{1}{2}(\cos\theta_r - \cos\theta_a)$.

3. Results and discussion

Equation (19) is solved numerically using an explicit finite difference scheme with central differences for the spatial terms and forward difference for the temporal term. An initial distribution of $\eta(r, 0)$ is assumed and the radius of the drop is assumed to be the location of $\eta = 0.5$. Equation (6) is then solved for a given volume and radius of the drop to obtain the contact angle. The contact angle is substituted in the Young's driving force H and the evolution equation (19) is solved. The domain size is chosen such that the drop remains far from the boundary and the boundary conditions do not influence the evolution of the drop. The thickness of the interface measured from $\eta = 0.95$ to $\eta = 0.05$ is approximately 2.5 μm (see Fig. S1 of the supporting material for a plot of an instantaneous solution of the phase field variable for gradient coefficient $\lambda = 1.8 \times 10^{-11}$ J). The grid size is chosen such that the interfaces contain at least 10 grid points.

Table 1
Line tension values for two different values of the gradient coefficient

λ	τ
1.8×10^{-11} J	3.82×10^{-7} N
3.6×10^{-11} J	5.42×10^{-7} N

Note that the line tension τ can only be calculated *a posteriori* since $\tau = \lambda\int_0^\infty(\partial\eta/\partial r)^2\,dr$ requires the solution to be known. Alternatively, the line tension has been determined from the slope of the cosine of the contact angle versus the curvature [49] (see Fig. S2 of the supporting material for a plot of the cosine of the equilibrium contact angle for two different values of λ). Since we are interested in solving for the equilibrium contact angle we set the rate-independent hysteresis parameter $\delta = 0$. The line tension values for two different values of the gradient coefficient λ are shown in Table 1. The line tension is in general a non-linear function of the gradient coefficient since the solution profile (and, thus, α) depends on the gradient coefficient.

Next we use the phase field theory to model the drop evolution experiment from Extrand [31]. We plot the hysteresis loops for two different materials: PFA and etched PFA (ePFA). We take the advancing and receding angles of PFA ($\theta_a^{\text{PFA}} = 107°$, $\theta_r^{\text{PFA}} = 84°$), and etched PFA ($\theta_a^{\text{ePFA}} = 67°$, $\theta_r^{\text{ePFA}} = 12°$) reported by Extrand [31]. The equilibrium contact angles ($\theta_Y^{\text{PFA}} = 95.4°$ and $\theta_Y^{\text{ePFA}} = 46.8°$) and the hysteresis parameter values ($\delta^{\text{PFA}} = 7.21$ J/m^2, $\delta^{\text{ePFA}} = 10.70$ J/m^2) are obtained from the experimental values of the advancing and receding angles following the procedure outlined above.

Figs. 2 and 3 are plots of the hysteresis loops of the contact angle vs the drop volume and the contact angle vs wetted circle radius respectively on smooth surfaces of PFA (loop ABCD) and etched PFA (loop PQRS) as the drop volume is cycled from 1 to 10 μl. A 1 μl drop is given an initial condition with a large radius and Eq. (19) is solved until a steady state for η is obtained (given by the condition $\int_A |\dot{\eta}|\,dA < \varepsilon$, where ε is a convergence criterion) to give the receding angle (point A). The drop volume is then incrementally increased and Eq. (19) is solved until the condition $\int_A |\dot{\eta}|\,dA < \varepsilon$ is satisfied. The contact angle increases at constant drop radius from A to B until the advancing angle is reached. If the drop volume was not incremented at any state between A and B, the drop would maintain its contact angle.

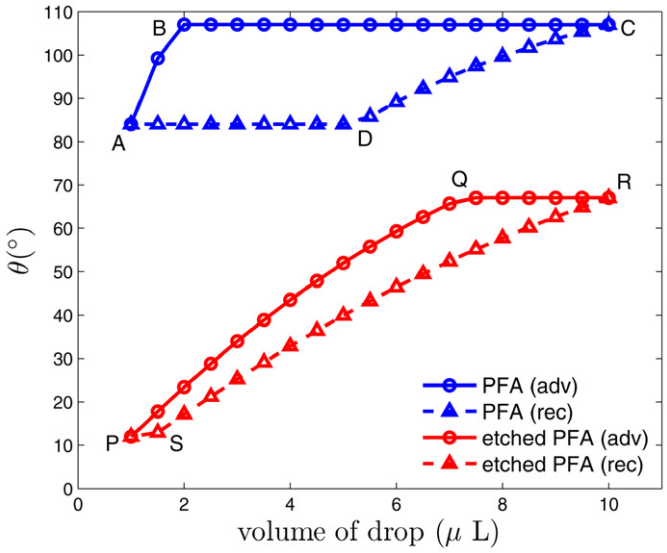

Fig. 2. Hysteresis loops for two surfaces with advancing and receding angles of PFA and etched PFA. The advancing drop is shown using circles and receding drop is shown using triangles.

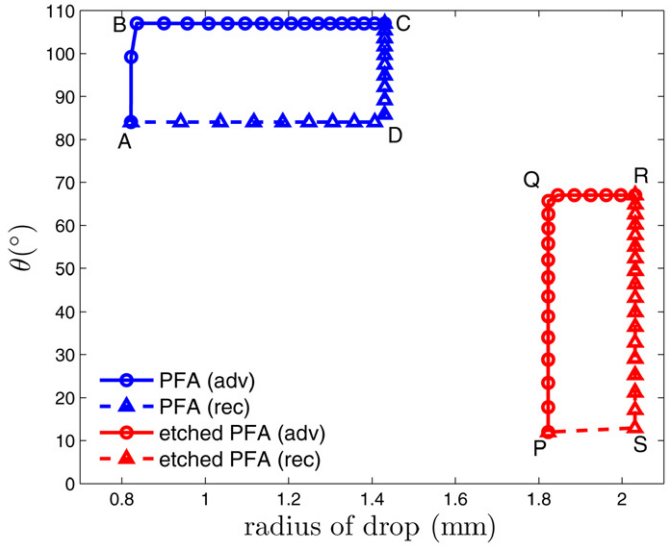

Fig. 3. Hysteresis loops for two surfaces with advancing and receding angles of PFA and etched PFA. The advancing drop is shown using circles and receding drop is shown using triangles.

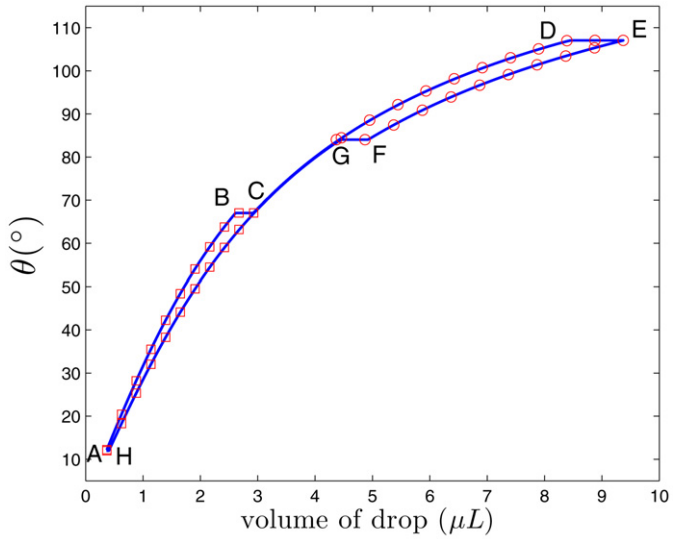

Fig. 4. Contact angle vs drop volume for a drop on a surface with a circular heterogeneity. The radius of the circular patch is $r = 1.35$ mm. The circles represent simulation results on a homogeneous PFA surface and the squares represent the simulation results on a homogeneous etched PFA surface.

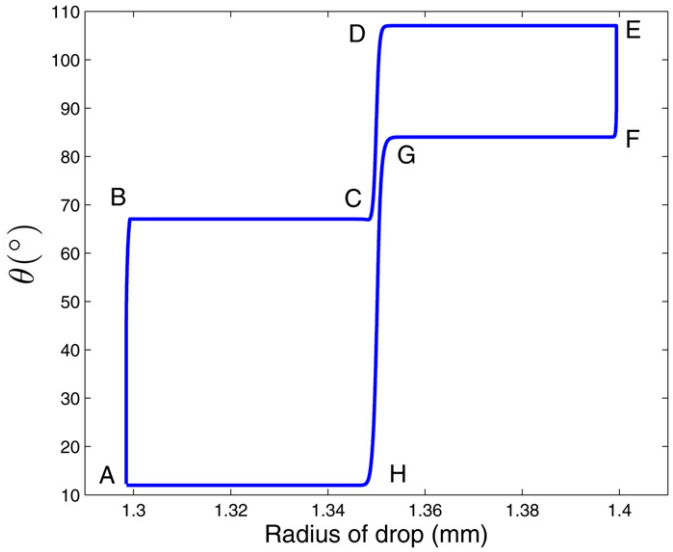

Fig. 5. Contact angle vs wetted circle radius for a drop on a surface with a circular heterogeneity. The radius of the circular patch is $r = 1.35$ mm.

In other words, all drop states between A and B are metastable. With further volume injection the contact angle remains constant at the advancing angle and the drop radius expands from B to C. The intermediate states from B to C are again metastable. When the volume of the drop reaches 10 μl, volume is withdrawn and the drop contact angle decreases at constant radius from C to D. Finally, when the contact angle attains the receding angle of the material, the drop radius decreases with decreasing volume from D to A.

When a drop wets a heterogeneous surface, the equilibrium contact angle on the composite surface is assumed to be related to the component surface equilibrium angles through the Cassie equation (3). It is also hypothesized that the advancing and receding angles of the composite surfaces are related to the advancing and receding angles of the component surfaces through equations analogous to the Cassie equation. However, recent experimental results of Extrand [31] show that the effective contact angle of the drop is determined by the surface properties experienced in the vicinity of the contact line. We study this situation by considering a surface of PFA in which a circular patch of radius $r = 1.35$ mm has been etched (Extrand [31]). A drop of volume 0.3 μl is placed inside the patch in a just receded state and volume is gradually injected up to 9.5 μl. The results of the simulations of contact angle vs drop volume and contact angle vs wetted circle radius are shown in Figs. 4 and 5, respectively. As the drop volume increases the contact angle increases from the receding angle to the advancing angle

on the etched PFA patch from A to B. This occurs at constant wetted circle radius. When the advancing angle is attained, the wetted circle radius begins to increase from B to C till the PFA surface in encountered at $r = 1.35$ mm. The contact angle then increases from C to D at this constant radius till the advancing angle of the PFA surface is attained. The wetted circle radius then increases at constant angle from D to E. Liquid is then withdrawn and the contact angle is observed to decrease till the receding angle of PFA is reached after which the wetted circle radius decreases till the etched PFA patch is encountered at G. The contact angle then decreases at constant radius till the receding angle of the etched PFA surface is attained at point H. For comparison, simulations results on homogeneous PFA and etched PFA are shown using circles and squares respectively in Fig. 4. The effect of the heterogeneous patch of the etched PFA is not observed in the loop DEFG. This is consistent with the experimental observations of Extrand [31].

As recognized by Cassie [3], the minimization of the free energy arises from the calculation of the *net change* in energy as a result of the advancing or receding process. The net change in energy per unit change in wetted area is computed as the difference between the energy gained by the destruction of the solid–air interfacial area and the energy that is expended in forming the solid–liquid interface over the same area [3]. When the contact line is wholly resident on the smooth PFA surface (with the etched PFA island entirely under the drop footprint) and acquires an incremental unit geometrical wetted area by advancement, all of the area acquired by the drop footprint is of material PFA. The net energy change for this event is only dependent on the properties of PFA and not of etched PFA. Therefore the appropriate area fractions to be used with Cassie's equation is $f^{\mathrm{PFA}} = 1$ and $f^{\mathrm{ePFA}} = 0$. When these values are used, Cassie equation yields the expected contact angle which is that of the smooth PFA. In contrast, an inappropriate choice of surface area fractions for this case would be based on the total geometric surface area fractions under the drop, given by $f^{\mathrm{PFA}} =$ (area of etched PFA)/(total solid–liquid interfacial area) and $f^{\mathrm{ePFA}} = 1 - f^{\mathrm{PFA}}$ [35]. The disagreement between Cassie theory and Extrand's [31] experiment arises from an incorrect choice of surface area fractions [50]. These observations are embodied in the phase field simulations since the evolution of the phase field variable occurs at the three-phase contact line following an energetically favorable path.

4. Summary

We have proposed a phenomenological model of wetting which is capable of characterizing sessile drop behavior through the constitutive parameters: θ_a, θ_r, γ_{LV}, τ. The behavior of the drop is shown to be determined by the material properties near the three-phase contact line in accord with the experimental observations of Extrand [31] and Gao and McCarthy [35]. To the best of our knowledge this is the first comprehensive phenomenological model of hysteresis in wetting. A significant advantage of this approach is that the individual origins of hysteresis are not explicitly taken into account. This allows the model to be applied to real surfaces on which multiple origins contribute to the overall hysteresis of the contact angle without the need to characterize either the roughness or chemical heterogeneities of the surface. While we presented the theory in the context of axisymmetric droplet wetting in one dimension in this paper, extension to surface heterogeneities in two dimensions [37] and other geometries poses no difficulty. We envisage applications of this model in design and detailed studies of heterogeneous surfaces, and in situations where the contact line effects are important [51].

Supplementary material

The online version of this article contains additional supplementary material.

Please visit DOI: 10.1016/j.jcis.2008.01.056.

References

[1] T. Young, Philos. Trans. R. Soc. London 95 (1805) 65.
[2] L. Boruvka, A.W. Neumann, J. Chem. Phys. 66 (1977) 5464.
[3] A.B.D. Cassie, Discuss. Faraday Soc. 3 (1948) 11.
[4] R.N. Wenzel, Ind. Eng. Chem. 28 (1936) 988.
[5] R.N. Wenzel, J. Phys. Colloid Chem. 53 (1949) 1466.
[6] P.G. de Gennes, Rev. Mod. Phys. 57 (1985) 827.
[7] H. Tavana, A.W. Neumann, Colloids Surf. A 282–283 (2006) 256, and references therein.
[8] X.F. Yang, Appl. Phys. Lett. 67 (1995) 2249.
[9] C.W. Extrand, J. Colloid Interface Sci. 207 (1998) 11.
[10] Y.L. Chen, C.A. Helm, J.N. Israelachvili, J. Phys. Chem. 95 (1991) 10736.
[11] C.W. Extrand, Y. Kumagai, J. Colloid Interface Sci. 191 (1997) 378.
[12] J.B. Freund, Phys. Fluids 15 (2003) L33.
[13] R.E. Johnson, R.H. Dettre, Contact Angle, Wettability and Adhesion, in: Advances in Chemistry, vol. 43, American Chemical Society, Washington, DC, 1964, p. 112.
[14] A. Marmur, Colloids Surf. A 136 (1998) 209, and references therein.
[15] C. Huh, S.G. Mason, J. Colloid Interface Sci. 53 (1977) 235.
[16] A.W. Neumann, R.J. Good, J. Colloid Interface Sci. 38 (1972) 341.
[17] J.D. Eick, R.J. Good, A.W. Neumann, J. Colloid Interface Sci. 53 (1975) 235.
[18] J.F. Joanny, P.G. de Gennes, J. Chem. Phys. 81 (1984) 552.
[19] Y. Pomeau, J. Vannimenus, J. Colloid Interface Sci. 104 (1985) 477.
[20] U. Opik, J. Colloid Interface Sci. 223 (2000) 143.
[21] J. Long, M.N. Hyder, R.Y.M. Huang, P. Chen, Adv. Colloid Interface Sci. 118 (2005) 173.
[22] V.M. Starov, M.G. Velarde, C.J. Radke, Wetting and Spreading Dynamics, Surfactant Science Series, vol. 138, CRC Press, 2007.
[23] L.W. Schwartz, Langmuir 14 (1998) 3440.
[24] S. Brandon, N. Haimovich, E. Yeger, A. Marmur, J. Colloid Interface Sci. 263 (2003) 237.
[25] Y. Chen, B. He, J. Lee, N.A. Patankar, J. Colloid Interface Sci. 281 (2005) 458.
[26] D. Chatain, D. Lewis, J.-P. Baland, W.C. Carter, Langmuir 22 (2006) 4237.
[27] C. Dorrer, J. Rühe, Langmuir 23 (2007) 3179.
[28] F. Porcheron, P.A. Monson, Langmuir 22 (2006) 1595.
[29] S. Kusumaatmaja, J.T. Yeomans, Langmuir 23 (2007) 6019.
[30] C. Priest, R. Sedev, R. Ralston, Phys. Rev. Lett. 99 (2007) 026103.
[31] C.W. Extrand, Langmuir 19 (2003) 3793.
[32] L. Gránásy, T. Pusztai, J.A. Warren, J. Phys. Condens. Matter 16 (2004) R1205.
[33] R. Ahluwalia, T. Lookman, A. Saxena, R.C. Albers, Acta Mater. 52 (2004) 209.
[34] M. Nosonovsky, Langmuir 23 (2007) 9919.
[35] L. Gao, T.J. McCarthy, Langmuir 23 (2007) 3762.
[36] F.E. Bartell, J.W. Shepard, J. Phys. Chem. 57 (1953) 455.
[37] S. Vedantam, M.V. Panchagnula, Phys. Rev. Lett. 99 (2007) 176102.

[38] E. Bormashenko, R. Pogreb, G. Whyman, M. Erlich, Langmuir 23 (2007) 6501.
[39] B. Bhushan, M. Nosonovsky, Y.C. Jung, J. R. Soc. Inter. 4 (2007) 643.
[40] K. Luo, M.-P. Kuittu, C. Tong, S. Majaniemi, T. Ala-Nissila, J. Chem. Phys. 123 (2005) 194702.
[41] T. Pompe, S. Herminghaus, Phys. Rev. Lett. 85 (2000) 1930.
[42] E. Fried, M.E. Gurtin, Physica D 72 (1994) 287.
[43] S.M. Allen, J.W. Cahn, Acta Metall. 27 (1979) 1085.
[44] E. Fried, Continuum Mech. Thermodyn. 9 (1997) 33.
[45] E. Fried, G. Grasch, Arch. Ration. Mech. Anal. 138 (1997) 355.
[46] E. Fried, SIAM J. Appl. Math. 66 (2006) 1130.
[47] S. Vedantam, Comput. Mech. 35 (2005) 369.
[48] S. Vedantam, Smart Mater. Struct. 15 (2006) 1172.
[49] A. Amirfazli, D.Y. Kwok, J. Gaydos, A.W. Neumann, J. Colloid Interface Sci. 205 (1998) 1.
[50] M.V. Panchagnula, S. Vedantam, Langmuir 23 (2007) 13242.
[51] N. Anantharaju, M.V. Panchagnula, S. Vedantam, S. Neti, S. Tatic-Lucic, Langmuir 23 (2007) 11673.